Sensitivity of Subsurface Ocean Temperature Variability to Specification of Surface Observations in the Context of ENSO

ARUN KUMAR

Climate Prediction Center, NOAA/NWS/NCEP, College Park, Maryland

CAIHONG WEN

Climate Prediction Center, NOAA/NWS/NCEP, College Park, and Innovim, Greenbelt, Maryland

YAN XUE AND HUI WANG

Climate Prediction Center, NOAA/NWS/NCEP, College Park, Maryland

(Manuscript received 14 November 2016, in final form 12 January 2017)

ABSTRACT

To estimate the state of the ocean in the context of monitoring and prediction, ocean analysis products combine observed information from various sources that include both in situ ocean measurements and estimates of atmospheric forcings derived either from numerical models or from objective analysis methods. In the context of El Niño–Southern Oscillation (ENSO) variability in the equatorial tropical Pacific, this study discusses two questions: 1) the role of surface forcings in resolving the observed variability of subsurface ocean temperatures, and 2) which component of surface forcings plays a more important role.

The analysis approach is based on ocean model simulations where specification of surface forcings is controlled and the resulting ocean state is either compared among various simulations or is compared with an independent ocean analysis (where information from in situ ocean temperature measurements is included). The results highlight the importance of the contribution of observed sea surface temperature (via its influence on surface winds due to coupled air–sea interactions) and the observed surface wind forcing in determining the evolution of subsurface ocean temperatures. Implications for assessing the feasibility of extending ocean analysis and forecasts back in time when in situ observations were limited are also discussed.

---

1. Introduction

Ocean data assimilation (ODA) systems are now routinely used for analyzing the state of the ocean in support of monitoring climate variability and for initializing predictions (e.g., Xue et al. 2012; Fujii et al. 2015). The observed data ingested in ODA systems include in situ ocean (e.g., ocean temperature and salinity) and atmospheric (e.g., surface winds, temperature, humidity, etc.) observations, among others.

Many of the ODA systems are generally used in conjunction with seasonal prediction efforts at present, and are commonly stand-alone ocean analysis systems (Xue et al. 2012) where the observed atmospheric variability is specified based on an independent atmospheric analysis. In this setup, surface wind stress and various components of heat and freshwater are an external forcing taken from an atmospheric analysis (and acts as a proxy for observed atmospheric information). In the ODA system, surface atmospheric forcing information and in situ ocean observations are used to generate an estimate of the ocean state.

Given multiple sources of observed information—surface forcing and ocean observations—that are used during ocean data assimilation, a question can be posed as to what is the relative contribution of surface forcings and in situ ocean observations in constraining the ocean state? In the context of the surface forcing alone, an additional question one can ask is what are the relative roles of various components of surface forcings—sea surface temperatures (SSTs), surface wind, heat and freshwater fluxes—in constraining the ocean state?

Corresponding author e-mail: Dr. Arun Kumar, arun.kumar@noaa.gov

Understanding the relative contribution from various sources of observed information used during ocean data assimilation is of importance under various contexts:

- In recent years, there have been increasing requirements for providing predictions at a longer lead time, for example, the decadal time scales (Meehl et al. 2014). Moreover, in the context of ENSO predictions, together with a desire to improve ENSO prediction skill, there is also a need to quantify the limits of ENSO predictability and low-frequency variations in its prediction skill (McPhaden 2012; Kumar et al. 2015). A useful way to validate seasonal and decadal prediction systems, and to understand low-frequency variability in prediction skill is to run the prediction system over as long a historical period as feasible. However, extending ocean predictions back in time is problematic because of the lack of subsurface ocean data that may be important for the specification of subsurface ocean state, which is important for seasonal and decadal prediction. Alternative strategies of ocean state estimation can be devised based on specification of surface forcings alone (Luo et al. 2005; Keenlyside et al. 2005; Servonnat et al. 2015; Zhu et al. 2015), the feasibility of which can be assessed by understanding the sensitivity of the ocean analysis to various components of the observing system. For example, in the equatorial Pacific, if specification of surface forcing alone can recover the subsurface variability that is most relevant for ENSO, then ocean analysis and ENSO prediction can be extended back in time even when subsurface observations themselves were not available.

- Over certain parts of the globe, for example, the equatorial tropical Pacific, the ocean and the atmospheric variability is strongly coupled. In such regimes, it is conceivable that because of strong coupling, specification of observed variability in one component may constrain and determine variability in the other component. An assessment of the relative importance of sensitivity in the ocean analysis to different observations, once again, will be helpful in assessing relative roles of different components of the observing system. The analysis is also of relevance in answering one of the scientific objectives of the recently launched Tropical Pacific Observing System 2020 (TPOS 2020) project (http://tpos2020.org/about/science-questions/): "To determine the most efficient and effective observational solutions to support prediction systems for ocean, weather and climate services."

- In the design of the ocean observing system, special attention needs to be paid in measuring those observable components of the ocean and atmosphere to

which the ocean state may be particularly sensitive. This aspect is important both for ocean state estimation and for focusing our attention on validating and improving the performance of the components of the atmospheric model (e.g., convection) to which the ocean is most sensitive.

With the goal to assess sensitivity in the ocean analysis to various sources of observed information—surface forcing and in situ ocean observations—we analyze a set of ocean-alone simulations. In these simulations, the extent of surface forcing information given to the ocean is controlled, and the simulated ocean state is compared among various simulations, and against an independent ocean analysis. Our analysis is in the context of the ocean observing system for ENSO monitoring and prediction, and therefore, the analysis focuses on the ocean variability in the equatorial tropical Pacific. Further, we focus on the analysis of variability in ocean temperature alone.

2. Ocean model simulations and analysis procedure

a. Ocean model simulations

The ocean model we used is the Geophysical Fluid Dynamics Laboratory Modular Ocean Model, version 4.1 (MOM4p1; Griffies 2010). The ocean model covers the global ocean from 80.75°S to 89.75°N, and has a zonal resolution of 0.5° and a meridional resolution of 0.25° between 10°S and 10°N, gradually increasing to 0.5° poleward of 30°S and 30°N. The MOM4p1 has 40 layers from 5 m below sea level to 4479 m, with a 10-m resolution in the upper 240 m. The MOM4p1 was forced by daily values of surface fluxes of momentum, net heat, and freshwater from atmospheric reanalysis products. The net heat flux is the sum of shortwave, longwave, and sensible and latent heat fluxes while components for freshwater flux include precipitation and evaporation.

To compensate for errors in the surface forcing and to avoid drifts, the ocean model temperature in the top level (5 m) was nudged to a daily OISST analysis (Reynolds et al. 2007) with a restoring time scale equivalent to 10 days. This procedure can also be thought of as a simple way to assimilate SST observations for which gridded estimates based on satellite retrievals and in situ measurements are widely available. The top-level salinity (5 m) was relaxed toward a seasonal climatology based on the *World Ocean Atlas (WOA) 1998* (Conkright et al. 1999) with a restoring time scale of 30 days. In contrast to the temperature in the top level of the ocean model, salinity was not nudged to its observational counterpart because gridded estimates of time-varying salinity are harder to come by.

TABLE 1. Summary of various ocean model simulations and surface forcings used.

Name of expt	Wind stress	Net heat flux	Freshwater flux [evaporation minus precipitation ($E - P$)]	Purpose
R2F	R2	R2	R2	Forced ocean simulation with R2 surface forcing and SST nudging
CFSRF	CFSR	CFSR	CFSR	Ocean simulation with CFSR surface forcing and SST nudging
R2F_CFSRW	CFSR	R2	R2	Influence of surface wind and SST nudging
R2F_CFSRHF	R2	CFSR	CFSR	Combined influence of surface heat and freshwater flux and SST nudging
R2F_CFSRH	R2	CFSR	R2	Influence of surface heat flux and SST nudging
R2_CFSRF	R2	R2	CFSR	Influence of freshwater flux and SST nudging
CLIM	Climatology	Climatology	Climatology	Forced ocean simulation with SST nudging and climatological surface forcing
CFSv2	—	—	—	Coupled simulation with SST nudging. Fluxes are computed internally

The model simulations were initiated from the GODAS ocean analysis (Behringer and Xue 2004) and were driven by daily values of surface fluxes from two different atmospheric reanalysis: the NCEP–DOE reanalysis (R2; Kanamitsu et al. 2002) and the Climate Forecast System Reanalysis (CFSR; Saha et al. 2010). Differences in surface forcings between R2 and CFSR, and ocean responses to respective forcings, quantify ocean sensitivity to the surface forcing.

To understand the sensitivity due to each flux component individually, four sensitivity experiments were also done by replacing R2 surface wind stress, heat, and freshwater fluxes by the corresponding fluxes in the CFSR. Table 1 describes the configuration of various MOM4p1 simulations. All experiments were run from the same initial conditions starting in January 1979. Considering the initial adjustment in the ocean model simulations, and to avoid issues reported in the abrupt discontinuity in the surface forcings for the CFSR (Kumar et al. 2012; Xue et al. 2011), we analyzed the simulations for the 1999–2013 period. To isolate the influence of SST nudging on the evolution of subsurface ocean temperatures, an additional experiment where surface forcings were specified as the daily climatology alone is also done. The daily climatology for respective forcings are constructed based on the R2 analysis. We note that the analysis reported in this paper does not include all simulations shown in Table 1, particularly with various combinations of replacing R2 surface forcings by their CFSR counterpart. This is because some of the sensitivity experiments do not add further to our conclusions, but for the sake of completeness are included in Table 1.

In addition to simulations described in Table 1, we also ran a coupled model simulation where surface forcings are no longer specified but are generated internally. During the coupled model integration,

however, the ocean model temperatures in the top level (5 m) were still nudged toward the observed SSTs. The purpose of this integration was to assess the extent to which the ocean state can be simulated from the specification (or assimilation) of the observed SSTs alone. In this simulation, the surface wind stress and heat and freshwater fluxes were not constrained to follow the observed variability as is the case for the other simulations described in Table 1. It is only the fraction of observed surface wind stress, heat, and freshwater fluxes that are constrained by the observed SST variability (due to ocean–atmospheric coupling) that are replicated in this simulation. The design of this simulation follows the one described in Wang et al. (2013) and Kumar et al. (2014).

b. Analysis procedures

Two approaches for analyzing ocean model simulations are pursued. In the first, interannual variability in ocean simulations with surface forcing from a different atmospheric analysis are compared. This comparison quantifies the sensitivity in the ocean state to uncertainty in surface forcing; however, this analysis does not compare the realism of the ocean state relative to observations. To further assess the relative importance in different components of surface forcings itself, comparisons of ocean simulations with controlled changes in surface forcing are also made (for different simulations, see Table 1).

In the second set of analyses the interannual variability in the ocean model simulations is assessed against an independent estimate of the observed ocean state. The intent of this set of analyses is to quantify the extent to which specification of surface forcing can also replicate the *observed* subsurface ocean variability. For regions where ocean simulations with the specification of surface forcing alone can mimic the observed subsurface

ocean state delineate the regions over which surface forcing is important in constraining the evolution of subsurface ocean temperatures. These are also the regions for which there is the potential that initialized ocean predictions can be extended farther back in time.

We note that we did not focus on the analysis of simulation of the mean ocean state because analysis of variability (and its differences among various simulations) is a more appropriate approach to address questions we raised in section 1. However, it is recognized that mean differences in R2 and CFSR fluxes can be substantial and can also lead to differences in the mean state of the ocean.

3. Results

We first quantify the consistency in the interannual variability of surface wind stress (SWS), surface heat, and freshwater fluxes between R2 and CFSR by computing the temporal correlations based on monthly mean anomalies over 1999–2013 (Fig. 1). Away from deep tropical latitudes, the anomaly correlation (AC) between R2 and CFSR SWS exceeds 0.9, indicating a good temporal consistency in the monthly mean interannual variability among the two analyses (Fig. 1a). Lower agreement is found in the deep tropics with the least agreement over the Atlantic where AC values as low as 0.4 occur. A similar latitudinal dependence for the consistency for net surface heat and freshwater flux also exists (Figs. 1b and 1c), however, the overall consistency for these is much lower than for the surface wind stress. Among the three quantities analyzed, the least level of consistency is for the freshwater flux, and is a result of either the differences in representing physical processes related to precipitation in models or is due to initial adjustments and drifts in atmospheric fields from the analyzed state during the assimilation cycle which can lead to large differences in precipitation estimates among different products (Zhang et al. 2012). We note that none of the quantities analyzed in Fig. 1 are direct observables that are assimilated but are estimates that are model-derived quantities.

Differences in surface forcings between R2 and CFSR provide a means to address how differences in the interannual variability of surface forcings influence the subsurface ocean variability in the ocean data assimilation, or alternatively, which differences in surface forcings have the strongest influence on the subsurface ocean variability.

To assess the sensitivity of subsurface ocean temperature variability to uncertainties in surface forcings, a comparison of the interannual variability in the thermocline depth (D20) is analyzed, and is shown in Fig. 2.
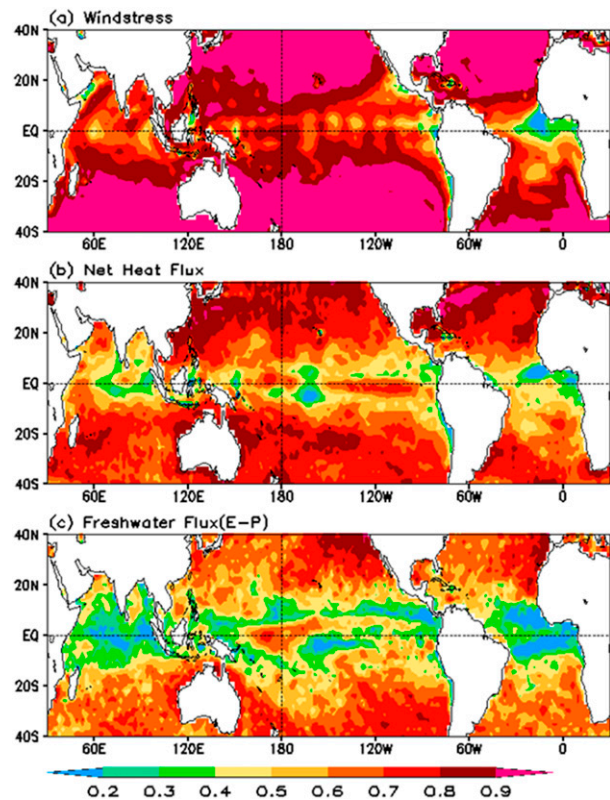

FIG. 1. Temporal anomaly correlation between monthly mean fields from the R2 and CFSR reanalysis for (a) surface wind stress, (b) net surface heat flux, and (c) net surface freshwater flux. The anomaly correlation is computed for the respective analysis over the 1999–2013 period.

The AC for D20 variability between ocean model simulations with surface forcing from R2 (R2F) and CFSR (CFSRF) (Fig. 2a) shows considerable spatial variability—higher correlations are found in the equatorial Indian and Pacific Oceans, with largest values east of the date line, a region where air–sea coupling associated with ENSO is strongest (Kumar and Hu 2014). Much smaller agreement in the simulation of D20 is found over the Atlantic as is generally also the case for current ODA systems (Zhu et al. 2012). We also note that the spatial distribution of high correlation for D20 between R2F and CFSRF matches well with the climatological variability of D20 (not shown) with regions of high (low) correlations coinciding with regions of high (low) seasonal variability in D20.

Which components of the surface forcings contribute to agreements and differences in the simulation of D20 can be inferred from sensitivity experiments where surface forcings from R2 and CFSR are interchanged in a controlled manner. D20 AC (Fig. 2b) between R2F and R2F_CFSRW (simulation where the SWS is from CFSR while heat and freshwater flux from R2 is used)
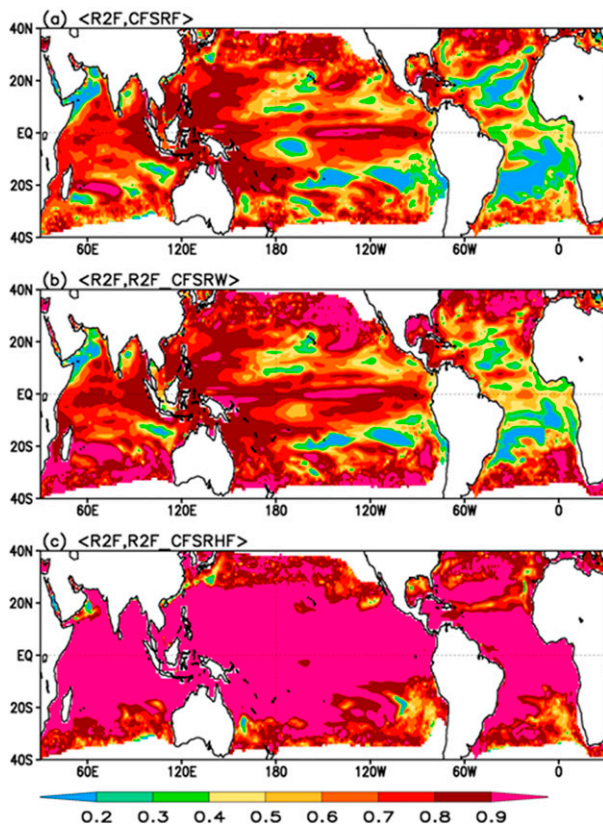
FIG. 2. Temporal anomaly correlation for D20 among ocean model simulations with different specification of surface forcings: (a) ocean model simulations with R2 and CFSR surface forcings; (b) ocean model simulations with R2 forcings, and with R2 forcings, but with surface wind stress from the CFSR; and (c) ocean model simulations with R2 forcings, and with R2 forcings, but with net heat flux forcing from the CFSR. The anomaly correlation is computed for the respective ocean model simulations over the 1999–2013 period.

shows a spatial distribution that is like that in Fig. 2a where respective forcing components from R2 and CFSR are used. This indicates that spatial differences in AC shown in Fig. 2a are mainly due to differences in the surface wind stress between R2 and CFSR, while contribution from surface heat and freshwater flux play a minor role. This is confirmed when R2F simulation is repeated but the heat and freshwater forcing is taken from the CFSR analysis (simulation R2F_CFSRHF in Table 1) and D20 AC throughout the tropical latitudes of the analysis domain is found to be very high (AC > 0.8) (Fig. 2c).

The results shown in Fig. 2 clearly indicate that on a monthly time scale, differences in the SWS influence the upper-ocean variability, while differences in heat and freshwater fluxes do not. This is consistent with the notion that the ocean is predominantly a wind-driven circulation. A caveat to note, however, is that the nudging

toward observed SST during simulations (and in ocean data assimilation) could dampen the influence of differences in heat fluxes. The influence of SST nudging alone is quantified based on the analysis of the CLIM simulations where variability in surface forcings is specified as its climatological seasonal cycle.

Besides the sensitivity to different components of surface forcings based on the analysis of comparison of various simulations, another analysis approach is to compare the simulations against the observed ocean variability and to assess what fraction of the observed subsurface variability can be recovered from the knowledge of surface forcings. For this, we compare the fidelity of simulations against observed ocean analysis based on EN4. We note that EN4 is an objective monthly analysis based on all in situ ocean observations (Good et al. 2013) and a comparison of model simulations (without inclusion of ocean data) with EN4 estimates the adequacy of surface forcings in constraining subsurface ocean temperature variability.

The fidelity of simulations against the variability in observed ocean analysis is quantified as the D20 temporal anomaly correlation. Figure 3 displays the spatial distributions of AC for R2F, R2F_CFSRW, and CFSv2 simulations. Regions with high (low) D20 AC are the regions where specification of surface forcing alone is able (unable) to recover the monthly mean observed subsurface ocean variability.

As indicated by large positive AC (>0.7) near the equatorial Pacific, a large fraction of the observed D20 variability can be recovered by the specification of SST and surface forcings (Fig. 3a for R2F and Fig. 3b for R2F_CFSRW simulation). Compared to R2F (Fig. 3a) the correlation is higher for the R2F_CFSRW simulation (Fig. 3b) in the eastern Pacific and near the date line, and is likely due to improved surface wind representation in the CFSR (Xue et al. 2011).

High correlations for R2F and R2F_CFSRW indicate that surface forcing can simulate subsurface ocean variability in the equatorial tropical Pacific. The same is not true for the tropical western Indian and Atlantic Oceans where low D20 ACs (<0.5) are found. This implies that specification of neither R2 nor CFSR surface forcing alone is sufficient to replicate the observed ocean state in these basins, and therefore, may point to the necessity of subsurface ocean observations to capture observed variability. It is also feasible that errors in the R2 and CFSR forcing may be at fault and improved specification of surface forcings may lead to better simulation of subsurface ocean variability. This question, however, cannot be resolved within the experimental setup used in our analysis.

In the model simulations in which specification of SST, surface wind, and heat and freshwater fluxes was
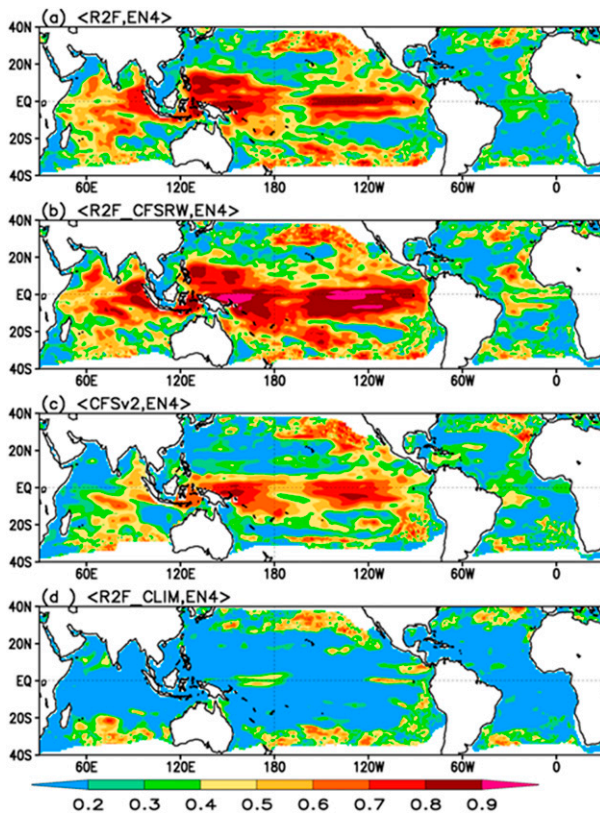
FIG. 3. Temporal anomaly correlation for D20 for various ocean model simulations and observed ocean analysis based on EN4: (a) ocean model simulation with R2 forcing; (b) ocean model simulations with R2 forcings, but with surface wind stress from the CFSR; (c) a coupled ocean model simulation with SST nudging, and (d) ocean model simulation with SST nudging and climatological surface forcings. The anomaly correlation is computed for the respective ocean model simulations over the 1999–2013 period.

included, what is the relative importance of the different components? From the discussions about Fig. 2 we had concluded that for D20 variability the role of heat and freshwater fluxes was not important. A question we next ask is what are the relative roles of SST and SWS in reproducing the observed subsurface ocean variability? To answer this question, we also included results from a CFSv2 simulation (Fig. 3c) in which during the simulation, only the observed SSTs are specified. As discussed earlier, in this simulation a part of the observed SWS variability is generated in response to SSTs, which in turn can influence subsurface ocean variability. Higher D20 AC in the equatorial tropical Pacific once again indicates that specification of SSTs, via coupled air–sea interactions, can recover subsurface ocean variability reasonably well (Kumar et al. 2014). The amplitude of AC, however, is generally lower than that for the simulations

(e.g., R2F_CFSRW) where observed surface wind variability is specified, and the difference between them indicates the contribution of the component-observed surface winds that is not replicated in the CFSv2 simulation.

The SWS in the coupled CFSv2 simulation can be separated into two components. One component is related to the response to specified SSTs while the other component is related to the atmospheric internal variability or the noise (Kirtman and Shukla 2002). While the component related to the SST response has a counterpart in the observations and can be quantified based on the temporal correlation between the surface winds in the CFSv2 simulations and observations (not shown) (see Kumar et al. 2014), the component related to atmospheric internal variability is random and will not have a temporal coherence between observations and the model simulation with specified SSTs. The added subsurface information in the R2F_CFSRW simulation, reflected as the higher D20 AC, comes from the specification of the component of the observed surface wind variability, which cannot be generated by the coupled air–sea interaction from the specification of SSTs.

In all the experiments discussed so far, the predicted sea surface temperatures were nudged toward the observations. In these simulations, it is possible that the vertical mixing in the upper oceans can itself be responsible for high D20 AC shown in Figs. 3a–c. To illustrate that merely specifying observed SSTs is not sufficient to generate the observed variability in the subsurface ocean temperature, and that the information about the SSW is also required (either via its specification from observations or generated via coupled air–sea interactions), D20 AC for the simulation where surface forcings are specified as their respective climatological value (the CLIM simulation in Table 1) is shown in Fig. 3d. Compared to the simulations where the SSW was either specified from observations or where it was generated internal to the coupled model simulation, D20 AC for the CLIM simulation is much lower. The results clearly indicate that high D20 ACs in Figs. 3a–c were not an artifact of nudging the predicted SSTs to observed values and observed SSW information is necessary.

To further confirm the differences in anomaly correlation in Fig. 3, we provide a detailed comparison of D20 variability among different simulations. The standard deviation of simulated monthly mean subsurface ocean temperature (SSOT) variability (averaged between 2°S and 2°N) among various simulations and for EN4 is shown in Fig. 4. For the EN4 the largest variability is along the thermocline (Fig. 4, purple line),
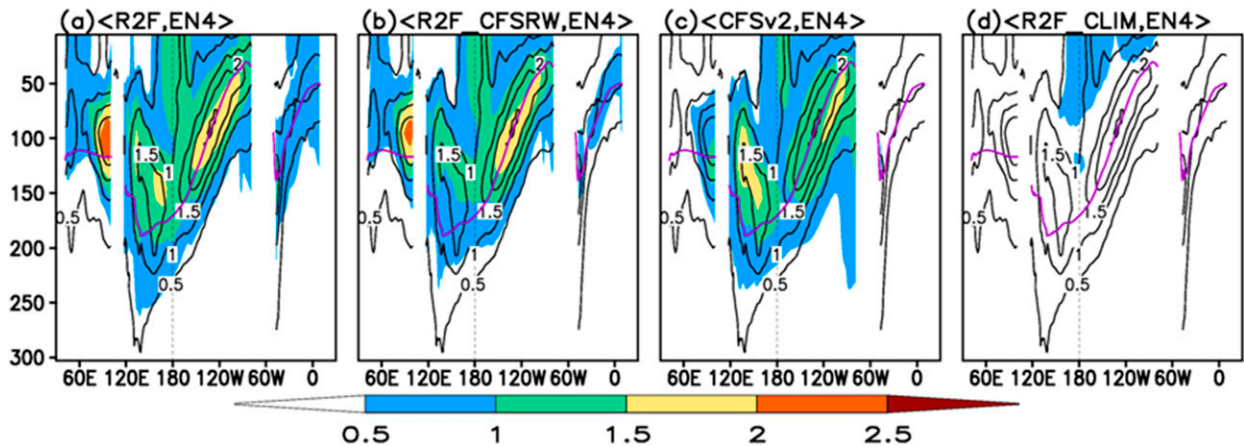
FIG. 4. Standard deviation of monthly mean subsurface ocean temperature averaged between 2°S and 2°N for (a) ocean model simulation with R2 forcing; (b) ocean model simulations with R2 forcings, but with surface wind stress from the CFSR; (c) a coupled ocean model simulation with SST nudging; and (d) ocean model simulation with SST nudging and climatological surface forcings. Shading is for model simulations; contours are for EN4. Units are in degrees squared. Purple lines denotes climatological mean of depth of 20°C in EN4.

and specifically in the tropical eastern Pacific (associated with ENSO) and in the eastern Indian Ocean (associated with the Indian Ocean dipole). Simulations where either SST or both the SST and surface forcings are specified replicate the observed SSOT variability well with maximum in variability located along the thermocline in the eastern Pacific and in the eastern Indian Ocean. In contrast, little SSOT variability in the CLIM simulation (where the interannual variability in surface forcings is not present) is found.

The evolution of D20 anomalies averaged between 2°S and 2°N for EN4 and for various simulations is shown in Fig. 5. For EN4 D20 anomalies follow the sequence of ENSO events with above- (below) normal anomalies in the eastern Pacific during El Niño (La Niña) and opposite sign anomalies in the western Pacific. Consistent with large positive D20 correlation for R2F, R2F_CFSRW, and CFSv2 simulations, the observed D20 variations found in the EN4 are well replicated. For the CLIM simulation, however, the observed D20 variations are not simulated at all. This once again highlights the importance of SWS either via its specification or via coupled air–sea interaction from the knowledge of sea surface temperatures.

To complement the analysis based on anomaly correlation to assess the fidelity in simulating the SSOT, we computed the root-mean-square error (RMSE). In contrast to the AC, which is a measure of phase relationship between two quantities, RMSE also measures the amplitude sensitivity. We computed the RMSE in the simulation of D20 relative to the observed variability over the analysis; however, the RMSE results in Fig. 6 are shown averaged between 2°S and 2°N, and for

reference, are compared with the standard deviation of observed D20.

Over the Pacific the D20 RMSE value for the ocean simulation are generally lower than the corresponding value for the observed standard deviation with lowest values for the R2F_CFSW for which the AC is also the largest (Fig. 3). A lower value of D20 of RMSE relative to its standard deviation is also consistent with the temporal evolution of D20 anomalies shown in Fig. 5. In the eastern Pacific, the largest RMSE value is for the CFSv2 simulation indicating that the specification of surface wind stress (as was the case for the R2F and the R2F_CFSW simulation) is important for the correct simulation of D20 variability. Over the Atlantic and the Indian Ocean, specification in SST or surface wind stress does not lead to D20 RMSE any lower than its standard deviation, and is consistent with Fig. 4 where small interannual variability in simulated D20 is found. An exception is the eastern Indian Ocean associated with the eastern component of the Indian Ocean dipole, also a region of strong air–sea coupling.

In the final analysis, we compare the simulated subsurface ocean temperature variability across a vertical cross section in the equatorial Pacific (Fig. 7). Consistent with the spatial map for D20, for R2F simulations SSOT AC is highest near the date line and extends up to the thermocline. Smaller correlations are found in the eastern Pacific, suggesting that in this region the observed SSOT variability is not as well replicated. The AC, however, improves for the R2F_CFSRW simulation, and as discussed, maybe a reflection of improved surface wind variability in the CFSR. Some positive correlations are also found for the CLIM simulation and
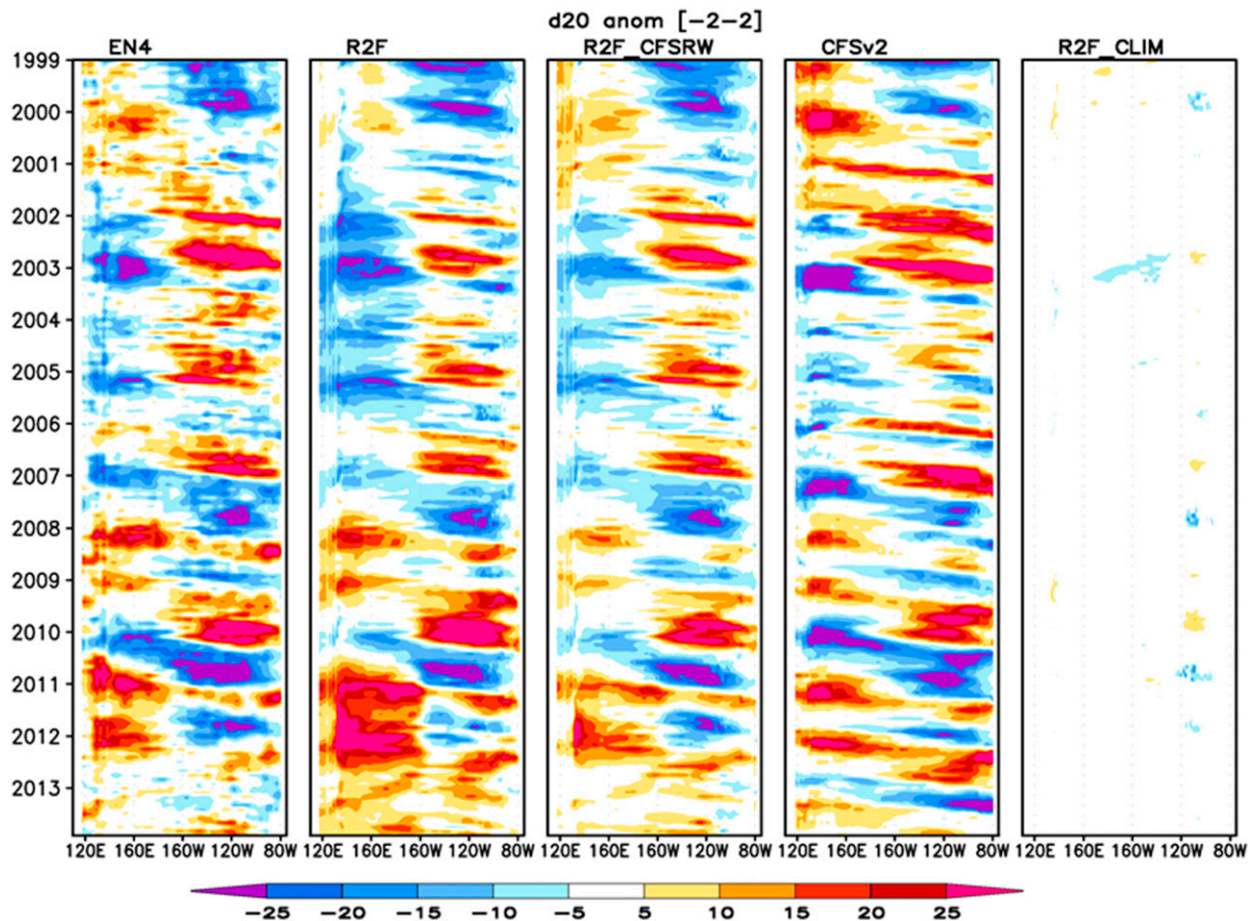
FIG. 5. Hovmöller of D20 anomaly for (from left to right) EN4; ocean model simulation with R2 forcing; ocean model simulations with R2 forcings, but with surface wind stress from the CFSR; a coupled ocean model simulation with SST nudging; and ocean model simulation with SST nudging and climatological surface forcings. Units are in meters. D20 is averaged between 2°S and 2°N.

are confined near the date line; however, they do not extend to the thermocline depth.

The results quantify the efficacy of specification of observed SSTs and surface winds in simulating observed subsurface ocean temperature variability on a monthly time scale. The combination of SST specification and surface wind stress better replicates observed ocean variability than the specification of SSTs alone (Fig. 4c for CFSv2 simulation), but nonetheless, observed SSTs alone, via coupled air–sea interaction can simulate subsurface ocean temperature variability.

4. Discussion

The analysis focused on the efficacy of surface ocean forcings and their ability in resolving subsurface temperature variability on a monthly time scale. Over certain oceanic regions, surface forcing is efficient in replicating the observed subsurface ocean temperature variability, and stems from coupled air–sea

interactions, which also give rise to predictability of SSTs on seasonal and longer time scales (e.g., ENSO). In a strongly coupled system, it is feasible that specification of one facet of the coupled system can also generate realistic variability in the other. For example, in the equatorial tropical Pacific, knowledge of SSTs, via coupled air–sea interactions, can lead to realistic simulation in surface wind variability, which in turn can result in realistic simulation of subsurface ocean temperatures. Indeed, and consistent with earlier results (Kumar et al. 2014; Servonnat et al. 2015; Zhu et al. 2015), it was shown that a specification of observed SSTs leads to a realistic simulation of subsurface temperature variability in the western and central Pacific (Fig. 4c). Specification of observed surface wind stress together with SSTs further improves the realism in the simulation of subsurface temperature variability. In the context of variability of ocean temperature, the analysis also documented the relative importance of surface wind stress versus heat
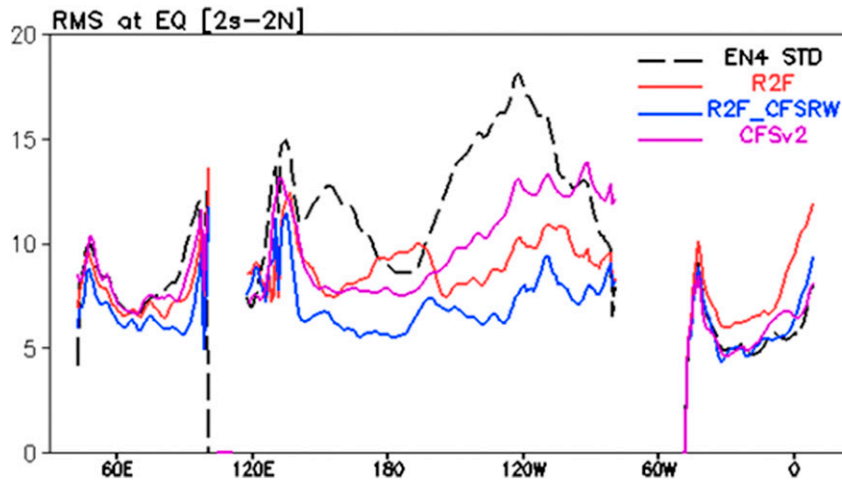
FIG. 6. Root-mean-square error (RMSE) for monthly mean D20 variability relative to EN4 for ocean model simulation with R2 forcing (red line); ocean model simulations with R2 forcings, but with surface wind stress from the CFSR (blue line); and a coupled ocean model simulation with SST nudging (purple line). For reference, the standard deviation of D20 variability in EN4 is shown in black line. RMSE is averaged between 2°S and 2°N. Units are in m^2.

and freshwater forcings in ocean data assimilation where information about SST is also assimilated.

The complementary nature of various observations over the regions of strong air–sea coupling can allow us to have some built in resiliency in the ocean observing system for monitoring and prediction of ENSO. Broadscale spatial observations for SSTs and winds in the equatorial Pacific are now routinely available via satellite, although errors in satellite estimates exist, particularly for the estimates of surface winds. The TAO moored array also provides high-quality surface wind observations. The subsurface ocean temperature variability inferred from these observations during data assimilation can complement the sparse network of in situ ocean observations available from XBT, TAO, and Argo, and provides an additional means to a better estimate of the ocean state and its evolution. That specification of surface forcings alone can also simulate realistic subsurface ocean temperature variability may also provide a means to extend ENSO predictions back in time even when subsurface observations themselves were sparse.
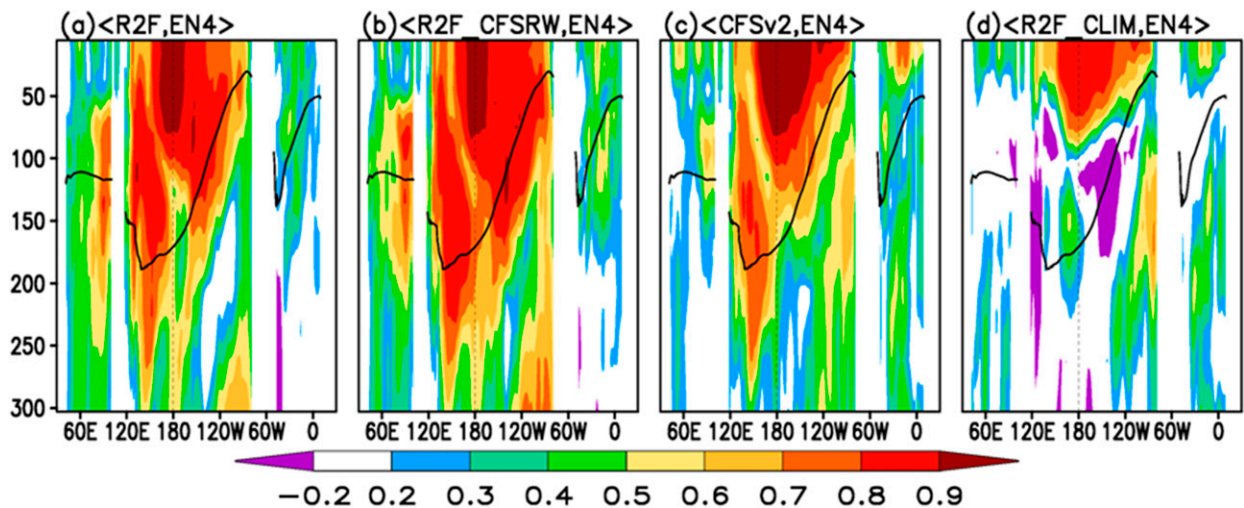

FIG. 7. As in Fig. 3, but for subsurface ocean temperature along the equator and averaged between 2°S and 2°N. Black lines denote climatological mean of depth of 20°C in EN4.

REFERENCES

Behringer, D., and X. Xue, 2004: Evaluation of the global ocean data assimilation system at NCEP: The Pacific Ocean. *Eighth Symp. on Integrated Observing and Assimilation Systems for Atmosphere, Oceans, and Land Surface*, Seattle, WA, Amer. Meteor. Soc., 2.3. [Available online at https://ams.confex.com/ams/pdfpapers/70720.pdf.]

Conkright, M. E., and Coauthors, 1999: World ocean database 1998, documentation and quality control version 2.0. National Oceanographic Data Center Internal Rep. 14, National Oceanographic Data Center, Silver Spring, MD, 127 pp. [Available online at ftp://ftp.nodc.noaa.gov/pub/data.nodc/woa/PUBLICATIONS/NODC_Internal_Rpt_14.pdf.]

Fujii, Y., and Coauthors, 2015: Evaluation of the Tropical Pacific Observing System from the ocean data assimilation perspective. *Quart. J. Roy. Meteor. Soc.*, **141**, 2481–2496, doi:10.1002/qj.2579.

Good, S. A., M. J. Martin, and N. A. Rayner, 2013: EN4: Quality controlled ocean temperature and salinity profiles and monthly objective analyses with uncertainty estimates. *J. Geophys. Res. Oceans*, **118**, 6704–6716, doi:10.1002/2013JC009067.

Griffies, S. M. 2010: Elements of MOM4p1. Tech. Rep. 6, NOAA/Geophysical Fluid Dynamics Laboratory, Princeton, NJ, 444 pp.

Kanamitsu, M., W. Ebisuzaki, J. Wollen, S. K. Yang, J. J. Hnilo, M. Fiorino, and G. L. Potter, 2002: NCEP–DOE AMIP-II reanalysis (R-2). *Bull. Amer. Meteor. Soc.*, **83**, 1631–1643, doi:10.1175/BAMS-83-11-1631.

Keenlyside, N. S., M. Latif, M. Botzet, J. Jungclaus, and U. Schulzweida, 2005: A coupled method for initializing El Niño–Southern Oscillation forecasts using sea surface temperature. *Tellus*, **57A**, 340–356, doi:10.1111/j.1600-0870.2005.00107.x.

Kirtman, B. P., and J. Shukla, 2002: Interactive coupled ensemble: A new coupling strategy for CGCMs. *Geophys. Res. Lett.*, **29**, 1367, doi:10.1029/2002GL014834.

Kumar, A., and Z.-Z. Hu, 2014: Interannual and interdecadal variability of ocean temperature along the equatorial Pacific in conjunction with ENSO. *Climate Dyn.*, **42**, 1243–1258, doi:10.1007/s00382-013-1721-0.

——, M. Chen, L. Zhang, W. Wang, Y. Xue, C. Wen, L. Marx, and B. Huang, 2012: An analysis of the nonstationarity in the bias of sea surface temperature forecasts for the NCEP Climate Forecast System (CFS) version 2. *Mon. Wea. Rev.*, **140**, 3003–3016, doi:10.1175/MWR-D-11-00335.1.

——, H. Wang, Y. Xue, and W. Wang, 2014: How much of monthly subsurface temperature variability in the equatorial

Pacific can be recovered by the specification of sea surface temperatures? *J. Climate*, **27**, 1559–1557, doi:10.1175/JCLI-D-13-00258.1.

——, M. Chen, Y. Xue, and D. Behringer, 2015: An analysis of the temporal evaluation of ENSO prediction skill in the context of the equatorial Pacific Ocean observing system. *Mon. Wea. Rev.*, **143**, 3204–3213, doi:10.1175/MWR-D-15-0035.1.

Luo, J.-J., S. Masson, S. Behera, S. Shingu, and T. Yamagata, 2005: Seasonal climate predictability in a coupled OAGCM using a different approach for ensemble forecasts. *J. Climate*, **18**, 4474–4497, doi:10.1175/JCLI3526.1.

McPhaden, M. J., 2012: A 21st century shift in the relationship between ENSO SST and warm water volume anomalies. *Geophys. Res. Lett.*, **39**, L09706, doi:10.1029/2012GL051826.

Meehl, G. A., and Coauthors, 2014: Decadal climate prediction: An update from the trenches. *Bull. Amer. Meteor. Soc.*, **95**, 243–267, doi:10.1175/BAMS-D-12-00241.1.

Reynolds, R. W., T. M. Smith, C. Liu, D. B. Chelton, K. S. Casey, and M. G. Schlax, 2007: Daily high-resolution blended analyses for sea surface temperature. *J. Climate*, **20**, 5473–5496, doi:10.1175/2007JCLI1824.1.

Saha, S., and Coauthors, 2010: The NCEP Climate Forecast System reanalysis. *Bull. Amer. Meteor. Soc.*, **91**, 1015–1057, doi:10.1175/2010BAMS3001.1.

Servonnat, J., J. Mingot, E. Guilyardi, D. Swingedouw, R. Seferiona, and S. Labetoulle, 2015: Reconstructing the subsurface ocean decadal variability using surface nudging in a perfect model framework. *Climate Dyn.*, **44**, 315–338, doi:10.1007/s00382-014-2184-7.

Wang, H., A. Kumar, and W. Wang, 2013: Characteristics of oceanic response to ENSO estimated from simulations with the NCEP Climate Forecast System. *J. Climate*, **26**, 8065–8083, doi:10.1175/JCLI-D-12-00795.1.

Xue, Y., B. Huang, Z.-Z. Hu, A. Kumar, C. Wen, D. Behringer, and S. Nadiga, 2011: An assessment of oceanic variability in the NCEP Climate Forecast System Reanalysis. *Climate Dyn.*, **37**, 2511–2539, doi:10.1007/s00382-010-0954-4.

——, and Coauthors, 2012: A comparative analysis of upper-ocean heat content variability from an ensemble of operational ocean reanalyses. *J. Climate*, **25**, 6905–6929, doi:10.1175/JCLI-D-11-00542.1.

Zhang, L., A. Kumar, and W. Wang, 2012: Influence of changes in observations on precipitation: A case study for the Climate Forecast System Reanalysis (CFSR). *J. Geophys. Res.*, **117**, D08105, doi:10.1029/2011JD017347.

Zhu, J., B. Huang, and M. A. Balmaseda, 2012: An ensemble estimation of the variability of upper-ocean heat content over the tropical Atlantic Ocean with multi-ocean reanalysis products. *Climate Dyn.*, **39**, 1001–1020, doi:10.1007/s00382-011-1189-8.

——, A. Kumar, H. Wang, and B. Huang, 2015: Sea surface temperature predictions in CFSv2 using a simple ocean initialization scheme. *Mon. Wea. Rev.*, **143**, 3176–3191, doi:10.1175/MWR-D-14-00297.1.